

Wide Operating Temperature Range Electrolytes for High Voltage and High Specific Energy Li-ion Cells

M. C. Smart¹, C. Hwang¹, F. C. Krause¹, J. Soler¹, W. C. West¹,
B. V. Ratnakumar¹, and K. Amine²

¹ Jet Propulsion Laboratory, California Institute of Technology,
Pasadena, California 91109-8099, USA

² Argonne National Laboratory,
9700 South Cass Avenue, Bld. 205, Argonne, IL 60439, USA

A number of electrolyte formulations that have been designed to operate over a wide temperature range have been investigated in conjunction with layered-layered metal oxide cathode materials developed at Argonne. In this study, we have evaluated a number of electrolytes in Li-ion cells consisting of Conoco Phillips A12 graphite anodes and Toda HE5050 $\text{Li}_{1.2}\text{Ni}_{0.15}\text{Co}_{0.10}\text{Mn}_{0.55}\text{O}_2$ cathodes. The electrolytes studied consisted of LiPF_6 in carbonate-based electrolytes that contain ester co-solvents with various solid electrolyte interphase (SEI) promoting additives, many of which have been demonstrated to perform well in 4V systems. More specifically, we have investigated the performance of a number of methyl butyrate (MB) containing electrolytes (i.e., LiPF_6 in ethylene carbonate (EC) + ethyl methyl carbonate (EMC) + MB (20:20:60 v/v %) that contain various additives, including vinylene carbonate, lithium oxalate, and lithium bis(oxalato)borate (LiBOB). When these systems were evaluated at various rates at low temperatures, the methyl butyrate-based electrolytes resulted in improved rate capability compared to cells with all carbonate-based formulations. It was also ascertained that the slow cathode kinetics govern the generally poor rate capability at low temperature in contrast to traditionally used $\text{LiNi}_{0.80}\text{Co}_{0.15}\text{Al}_{0.05}\text{O}_2$ -based systems, rather than being influenced strongly by the electrolyte type.

Introduction

The Department of Energy (DoE) is interested in developing more efficient energy storage technologies to enable plug-in hybrid electric vehicles (PHEVs) to meet the desired electric mileage ranges. To meet these objectives, many groups have been developing high voltage, high capacity cathode materials to improve the specific energy over the current Li-ion technology. NASA also has interest in higher specific energy rechargeable batteries, especially for “human rated” applications. Argonne has developed a number of lithium-excess layered-layered metal oxide materials, which are composites

of $x\text{Li}_2\text{MnO}_3-(1-x)\text{LiMO}_2$ ($M=\text{Mn, Co, Ni}$), that have been demonstrated to provide over 250 mAh /g in many cases.¹⁻⁴ Although these materials have been demonstrated to provide excellent specific capacity when cycled over a wide voltage range (i.e., 2.0 to 4.80V vs. Li^+/Li), a number of technical challenges need to be overcome prior to its widespread adoption, including improving the rate capability of material and demonstrating the life characteristics when coupled with relevant carbon-based anodes. In addition, very few studies have addressed the capability of the material to operate over a wide temperature range, especially at lower temperatures.

In the current study, we have investigated a number of electrolyte formulations that have been designed to operate over a wide temperature range in conjunction with the layered-layered metal oxide cathode material developed at Argonne. Specifically, we have evaluated a number of electrolytes in Li-ion cells consisting of Conoco Phillips A12 graphite anodes and Toda HE5050 $\text{Li}_{1.2}\text{Ni}_{0.15}\text{Co}_{0.10}\text{Mn}_{0.55}\text{O}_2$ cathodes (developed by Argonne). The electrolytes studied consisted of LiPF_6 in carbonate-based electrolytes that contain ester co-solvents with various solid electrolyte interphase (SEI) promoting additives, many of which have been demonstrated to perform well in lower voltage systems.^{5,6,7} For instance, we have investigated the performance of a number of methyl butyrate (MB) containing electrolytes (i.e., LiPF_6 in ethylene carbonate (EC)+ ethyl methyl carbonate (EMC) + MB (20:20:60 v/v%) that contain various additives, including vinylene carbonate, **1**, lithium oxalate, **2**, and LiBOB , **3**, the structures of which are shown in Figure 1.

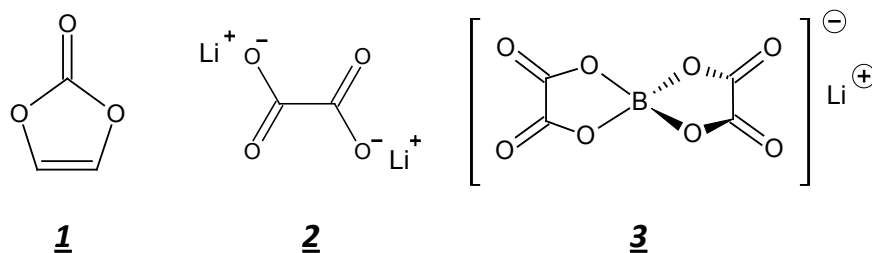


Figure 1. Chemical structures of various electrolyte additives investigated in conjunction with methyl butyrate-based wide operating temperature range lithium-ion battery electrolytes, including vinylene carbonate (VC), **1**, lithium oxalate, **2**, and lithium bis(oxalato)borate, **3**.

In contrast to the bulk of the studies performed on the layered-layered composite metal oxide materials which have been evaluated against lithium metal, the current study was performed with electrochemically matched carbon anodes (graphite). In addition to evaluating the discharge rate capacity and the cycle life performance in a number of coin cells (CR2032 size), larger capacity three-electrode cells (equipped with lithium metal references electrodes) were utilized to study the lithium kinetics of the respective electrodes by electrochemical techniques. In particular, both anodes and cathodes were subjected to a number of electrochemical measurements, including Electrochemical Impedance Spectroscopy (EIS), Tafel polarization, and linear micro-polarization measurements. These measurements were performed at different temperatures to determine the relative kinetics, especially at low temperatures. Upon performing Tafel polarization measurements on each electrode (which possess relatively heavy loadings), it was observed that the HE5050 cathode displayed poor lithium kinetics (limiting

electrode) compared to the anode. Further, EIS measurements suggest that the charge-transfer kinetics of the cathode contributes significantly to the overall cell impedance and poor rate capability. When the cells were evaluated at various rates at low temperatures, the methyl butyrate-based electrolytes resulting in improved rate capability compared to a cell with an all carbonate-based formulation. However, based on the results obtained from Tafel polarization and EIS measurements, it appears as though the cathode kinetics is dominating the generally poor rate capability at low temperature rather than the electrolyte type. In addition to investigating wide operating temperature range electrolytes, some effort was devoted to evaluating electrolytes with flame retardant additives^{8,9} in conjunction with the high voltage system to demonstrate their compatibility, which will be communicated in a future publication.

Experimental

For detailed electrical and electrochemical measurements, three-electrode, O-ring sealed, glass cells containing spiral rolls of Conoco Phillips A12 graphite anodes, Toda HE5050 $\text{Li}_{1.2}\text{Ni}_{0.15}\text{Co}_{0.10}\text{Mn}_{0.55}\text{O}_2$ (NCM) or $\text{LiNi}_{0.80}\text{Co}_{0.15}\text{Al}_{0.05}\text{O}_2$ (NCA) cathodes, and lithium reference electrodes separated by two layers of porous polyethylene (20 μm Tonen-Setella separator) were employed. The Conoco Phillips A12 graphite anode electrodes ($\sim 39 \mu\text{m}$ coating thickness) were coated with active material on both sides of the substrate and had an active material area of approximately 158.1 cm^2 , corresponding to $\sim 6.1 \text{ mg/cm}^2$. The NCM cathode electrodes ($\sim 35 \mu\text{m}$ coating thickness) and the NCA cathode electrodes ($\sim 43 \mu\text{m}$ coating thickness) were also double sided with an active material area of approximately 141.1 cm^2 , corresponding to $\sim 7.6 \text{ mg/cm}^2$ and $\sim 11.45 \text{ mg/cm}^2$, respectively. The active material weight percent of both the $\text{Li}_{1.2}\text{Ni}_{0.15}\text{Co}_{0.10}\text{Mn}_{0.55}\text{O}_2$ (NCM) and $\text{LiNi}_{0.80}\text{Co}_{0.15}\text{Al}_{0.05}\text{O}_2$ (NCA) electrodes were 86%, and the active material weight percent of the graphite anodes was 87%. Coin cell studies were performed with the $\text{Li}_{1.2}\text{Ni}_{0.15}\text{Co}_{0.10}\text{Mn}_{0.55}\text{O}_2$ (NCM) and Conoco Phillips A12 graphite anodes electrodes by assembling them in stainless steel CR2032 coin cell hardware with Al clad stainless steel cases. The carbonate-based solutions, ethylene carbonate (EC) and ethyl methyl carbonate (EMC) containing LiPF_6 salt in the desired concentration, were purchased from Novolyte, Inc. and contained less than 50 ppm of water. Purified methyl butyrate (MB), and additional LiPF_6 salt were also procured from Novolyte, Inc. and added to the stock solutions to produce the desired formulations.

Electrochemical measurements were made using an EG&G Potentiostat/Galvanostat (273A) interfaced with an IBM PC, using Softcorr 352. A Solartron 1255 Frequency Response Analyzer was used with this potentiostat for impedance measurements, with M388 software. Charge-discharge measurements and cycling tests were performed with either an Arbin battery cycler or a Maccor battery test system. The cycling tests were performed using $\sim C/10$ or $\sim C/20$ rates for charge and discharge. The cells were charged to 4.55 V or 4.10V for $\text{Li}_{1.2}\text{Ni}_{0.15}\text{Co}_{0.10}\text{Mn}_{0.55}\text{O}_2$ (NCM) and $\text{LiNi}_{0.80}\text{Co}_{0.15}\text{Al}_{0.05}\text{O}_2$ (NCA) systems, respectively, followed by a tapered charge period until the current decayed to less than $C/50$, and then discharged to 2.50 V following a 15 minute rest interval. For the low temperature discharge rate characterization of the experimental cells, after charging at room temperature, the cells were allowed to dwell at the desired temperature for at least 5 hours prior to discharging to 2.50 V. To maintain the cells at the desired temperature, they were placed in Tenney environmental chambers ($\pm 1^\circ\text{C}$).

Results and Discussion

As mentioned previously, we have investigated the performance of ester-based wide operating temperature range electrolytes in the context of high voltage systems, namely the excess lithium layered-layered composite oxides $\text{Li}_{1.2}\text{Ni}_{0.15}\text{Co}_{0.10}\text{Mn}_{0.55}\text{O}_2$ (NCM) developed by Argonne. In particular, we have studied a number of methyl butyrate-based electrolytes (with various additives, including vinylene carbonate, lithium oxalate, and LiBOB) in three-electrode cells consisting of Conoco graphite anodes and NCM cathodes. We have also investigated the behavior of an all-carbonate based electrolyte in this system as well to serve as a baseline (e.g., DoE baseline electrolyte), to enable us to ascertain the performance of the methyl butyrate electrolytes. Furthermore, we have studied the performance of the one of the MB-based electrolytes in a graphite/NCA cell to enable the direct comparison of the cathode kinetics. In summary, the electrolytes investigated in these three-electrode cells include the following:

- 1.2 M LiPF_6 in EC+EMC (30:70 v/v %)
- 1.0 M LiPF_6 in EC+EMC+MB (20:20:60 v/v %) + 0.10M LiBOB
- 1.0 M LiPF_6 in EC+EMC+MB (20:20:60 v/v %) + 2 % VC
- 1.0 M LiPF_6 in EC+EMC+MB (20:20:60 v/v %) + lithium oxalate (~1%)

Since these cells are equipped with lithium reference electrodes, it enables the lithium kinetics to be studied of the respective electrodes by electrochemical techniques. Thus, in addition to characterizing the cells in terms of their charge/discharge performance, both anodes and cathodes were subjected to a number of electrochemical measurements, including Electrochemical Impedance Spectroscopy (EIS), Tafel polarization, and linear micro-polarization measurements, as described below.

Formation Characteristics of Graphite/ NCM and Graphite/NCA Three-Electrode Cells.

As illustrated in Figure 2, the graphite/NCM three-electrode cells were subjected to formation conditions consisting of using a C/20 charge rate to 4.55V (with a C/50 taper current cut-off) and a C/20 discharge rate to 2.50V. With the benefit of having a lithium metal reference electrode, the anode and cathode potentials were monitored throughout the cycling tests. As evidenced by the voltage response of the respective electrodes, the cathode and anode were relatively well matched. For example, upon the first charge the lowest voltage observed for the anode was 0.066V versus Li^+/Li , whereas the highest voltage for the cathode was 4.634V versus Li^+/Li . Upon analyzing the fifth discharge, the highest voltage observed for the anode was 0.699V versus Li^+/Li , whereas the lowest voltage exhibited by the cathode was 3.199V versus Li^+/Li . These results suggest that in this particular cell design (i.e., the ratio of cathode to anode capacities) that somewhat lower specific capacities of the cathode will be observed compared to Li/NCM “half” cells, where full utilization of the cathode can be obtained. Enhanced utilization of the cathode can also be accomplished by increasing the proportion of the graphite anode, which will result in lower end of discharge (lithium de-intercalation) anode potentials.

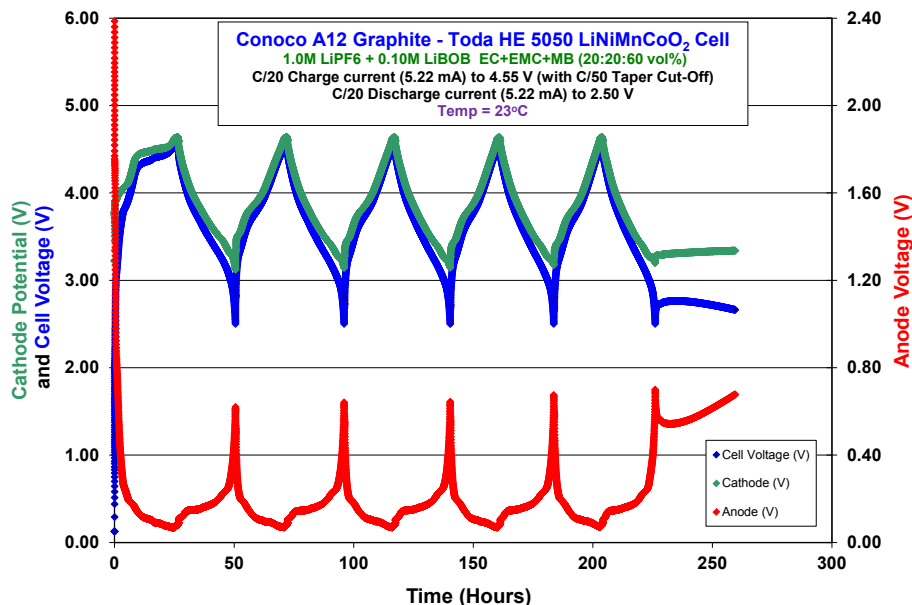


Figure 2. Formation characteristics of a graphite/ $\text{Li}_{1.2}\text{Ni}_{0.15}\text{Co}_{0.10}\text{Mn}_{0.55}\text{O}_2$ (NCM) cell containing 1.0M LiPF_6 + 0.10M LiBOB in EC+EMC+MB (20:20:60 v/v %) at 23°C using a C/20 charge rate to 4.55 V and a C/20 discharge rate to 2.50 V.

When the formation characteristics for three graphite/ $\text{Li}_{1.2}\text{Ni}_{0.15}\text{Co}_{0.10}\text{Mn}_{0.55}\text{O}_2$ (NCM) cells containing methyl butyrate-based electrolytes with various additive are compared, as shown in Table 1, the cell containing lithium oxalate delivered the highest reversible cathode specific capacity (i.e., 257 mAh/g) at the end of the five formation cycles and the lowest cumulative irreversible capacity (125 mAh/g for the combined anode and cathode). The use of lithium oxalate was originally conceived to complex any free PF_5 generated from the decomposition of LiPF_6 ^{7,10} much in the same manner as LiBOB has been reported to stabilize LiPF_6 -based solutions.¹¹ In contrast, the cell containing VC as an electrolyte additive displayed the lowest reversible cathode specific capacity (i.e., 224 mAh/g) and highest cumulative irreversible capacity (212 mAh/g). As mentioned above, some differences in the reversible cathode capacity may be observed amongst the cells depending upon the extent to which the anode is utilized. It should also be noted that these three-electrode cells represent a flooded electrolyte design, so the absolute amount of a sacrificial additives (such as vinylene carbonate) will be greater than in an electrolyte starved cell design. This suggests that further optimization of the electrolyte concentration may be warranted depending upon the test vehicle in which the solution is being investigated. As expected, the cell possessing the NCA cathode instead of the NCM cathode displayed much lower reversible specific cathode capacity (i.e., 154 mAh/g) and lower cumulative irreversible capacity. As reported, the high irreversible capacity of the NCM materials is primarily due to oxygen release from the cathode during the first cycle at the voltage plateau corresponding to 4.5V versus Li^+/Li in the first charge, and the accompanying diffusion of transition metal ions from the surface to the bulk where they occupy vacancies that are created by the removal of lithium.¹² To date, it is unclear what contribution that electrolyte composition plays in influencing this

particular mechanism of irreversible capacity loss, however, it is generally agreed that the electrolyte type can have a dramatic role upon the nature of the cathode electrolyte interface (CEI) and subsequently the resulting lithium kinetics.

Table 1. The formation characteristics of graphite/ NCM and graphite/ NCA cells containing methyl butyrate-based electrolyte at 23°C using a C/20 charge rate to 4.55 V and a C/20 discharge rate to 2.50 V.

Electrolyte Type	Charge Capacity (mAh/g) 1st Cycle	Discharge Capacity (mAh/g) 1st Cycle	Irreversible Capacity (mAh/g) (1st Cycle)	Coulombic Efficiency (1st Cycle)	Reversible Capacity (mAh/g) 5th Cycle	Cummulative Irreversible Capacity (mAh/g) (1st-5th Cycle)	Cathode Type
1.0M LiPF ₆ + 0.10M LiBOB EC+EMC+MB (20:20:60 vol%)	323.57	246.10	77.47	76.06	243.87	138.98	Argonne NMC (Toda HE 5050)
1.0M LiPF ₆ EC+EMC+MB (20:20:60 vol%) + 1.5% VC	325.89	233.46	92.43	71.64	224.33	211.93	Argonne NMC (Toda HE 5050)
1.0M LiPF ₆ EC+EMC+MB (20:20:60) + lithium oxalate	337.29	261.84	75.45	77.63	257.10	125.28	Argonne NMC (Toda HE 5050)
1.0M LiPF ₆ + 0.10M LiBOB EC+EMC+MB (20:20:60 vol%)	182.62	161.05	21.57	88.19	153.90	91.64	Argonne NCA (LiNiCoAlO ₂)

Discharge Characteristics of Graphite/ NCM and Graphite/NCA Three-Electrode Cells.

After completing the formation cycles and performing the electrochemical characterization (i.e., Tafel polarization and EIS measurements described in the sections below), the cells were subjected to discharge rate characterization as a function of temperature. As summarized in Table 2, the cells were discharged at various rates (i.e., C/20, C/10, C/5 and C/2) and at different temperature (20°, 10°, and 0°C). Prior to each discharge at low temperature the cells were charged at room temperature. In addition to assessing the methyl butyrate containing electrolytes described previously, a baseline all-carbonate-based electrolyte was evaluated as well, namely 1.2M LiPF₆ in EC+EMC (30:70 v/v %). At 20°C, the cell containing the baseline all carbonate electrolyte displayed the highest capacity at low to moderate rates. However, at lower temperatures especially at higher rates, the methyl butyrate-based electrolytes displayed much better capacity retention and discharge rate capability. For example, at 0°C the following trend was observed in terms of capacity delivered at a C/2 discharge rate (as expressed in terms of cathode specific capacity): EC+EMC+MB + 0.10M LiBOB (109 mAh/g) > EC+EMC+MB + lithium oxalate (74 mAh/g) > EC+EMC+MB + lithium oxalate (52 mAh/g) > EC+EMC (29 mAh/g), as displayed in Figure 3A. When the cells were evaluated at -20°C using a moderate discharge rate (C/10), a similar trend in performance was observed, with the cell containing the 1.0 M LiPF₆ + 0.10M LiBOB in EC+EMC+MB (20:20:60 v/v %) electrolyte exhibiting the best performance, as shown in Figure 3B. The improved performance of the cells containing methyl butyrate-based solutions at low temperatures compared to the all-carbonate formulation can be rationalized in part by the higher ionic conductivity of the electrolytes, resulting from the addition of the low viscosity co-solvent. The superiority of the blend containing LiBOB as an additive suggests that the cathode kinetics have been improved in this system by interacting in the formation of a desirable cathode electrolyte interface (CEI), which is supported by the results of the electrochemical characterization discussed below.

Table 2. The discharge characteristics of graphite/ NCM cells containing methyl butyrate-based electrolyte at 23°C using a C/20 charge rate to 4.55 V and a C/20 discharge rate to 2.50 V.

Electrolyte Type		1.0M LiPF ₆ + 0.10M LiBOB EC+EMC+MB (20:20:60 vol%)			1.0M LiPF ₆ EC+EMC+MB (20:20:60 vol%) + 1.5% VC			1.0M LiPF ₆ EC+EMC+MB (20:20:60) + lithium oxalate			1.2M LiPF ₆ EC+EMC (30:70 vol%)		
Temperature	Current (mA)	Capacity (Ahr)	Capacity (mAh/g)	Percent (%)	Capacity (Ahr)	Capacity (mAh/g)	Percent (%)	Capacity (Ahr)	Capacity (mAh/g)	Percent (%)	Capacity (Ahr)	Capacity (mAh/g)	Percent (%)
23°C	C/20	0.1100	243.87	100.00	0.1018	224.33	100.00	0.1168	257.10	100.00	0.1211	266.57	100.00
	C/10	0.1059	234.95	96.34	0.1001	220.53	98.31	0.1130	248.60	96.69	0.1108	243.84	91.47
	C/5	0.0973	215.91	88.54	0.0947	208.66	93.01	0.1039	228.57	88.90	0.1029	226.42	84.94
	C/2	0.0843	186.92	76.65	0.0840	185.03	82.48	0.0900	197.97	77.00	0.0896	197.16	73.96
10°C	C/20	0.0972	215.59	88.40	0.0829	182.73	81.45	0.0974	214.33	83.37	0.1037	228.15	85.58
	C/10	0.0911	201.99	82.82	0.0798	175.82	78.37	0.0894	196.81	76.55	0.0858	188.84	70.84
	C/5	0.0798	177.06	72.60	0.0717	158.05	70.46	0.0798	175.55	68.28	0.0599	131.77	49.43
	C/2	0.0636	141.14	57.88	0.0526	116.01	51.71	0.0585	128.72	50.07	0.0335	73.81	27.69
0°C	C/20	0.0848	187.98	77.08	0.0668	147.14	65.59	0.0808	177.86	69.18	0.0748	164.70	61.78
	C/10	0.0745	165.15	67.72	0.0559	123.14	54.89	0.0670	147.33	57.30	0.0349	76.85	28.83
	C/5	0.0646	143.21	58.72	0.0467	102.91	45.88	0.0559	123.02	47.85	0.0250	55.12	20.68
	C/2	0.0491	108.92	44.66	0.0235	51.71	23.05	0.0334	73.53	28.60	0.0130	28.57	10.72

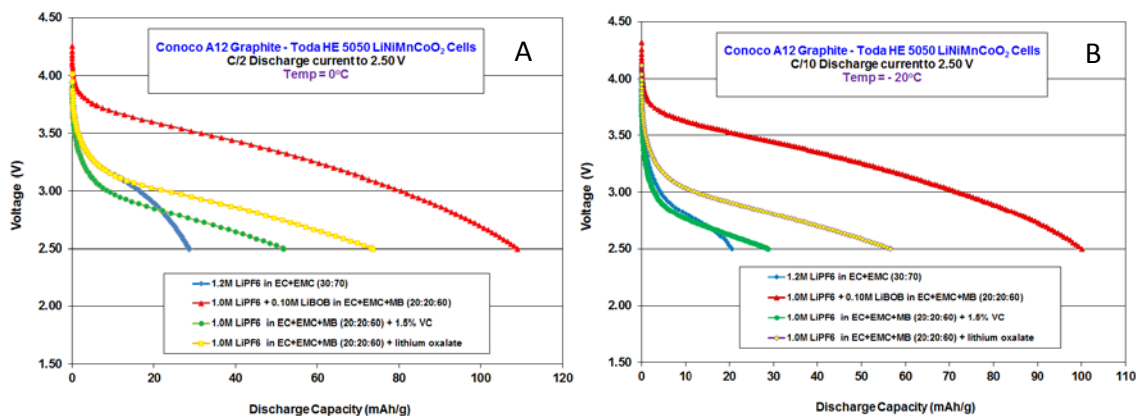


Figure 3. Discharge performance (expressed in terms cathode specific capacity) of graphite/ NCM cells containing methyl butyrate-based electrolytes at (A) 0°C using a C/2 discharge rate and at (B) -20°C using a C/10 discharge rate to 2.50 V. Cells were charged at room temperature to 4.55V prior to discharge.

Tafel Polarization Measurements of Graphite/ NCM and Graphite/NCA Cells.

Tafel polarization measurements on each electrode at a number of temperatures (20°, 0°, and -20°C) were performed to determine the relative lithiation/de-lithiation kinetics, in an attempt to ascertain the rate limiting electrode. These measurements were taken after charging the cells fully (to 4.55V) and were performed under potentiodynamic conditions, using slow scan rate to approximate steady-state conditions (i.e., 0.20mV/sec). In general,

both the NCA and NCM electrodes displayed poorer lithium kinetics (i.e., the rate limiting electrode) compared to the anode. When the cathode measurements were performed at 0°C, as illustrated in Fig. 4, the NCM electrodes displayed much lower lithium intercalation kinetics compared to the NCA electrodes (attributed to poor charge transfer resistance of the electrodes), which is exacerbated at lower temperatures. Of the NMC-based cells, the electrolyte containing LiBOB resulted in the most favorable lithium de-intercalation kinetics, illustrating the that the nature of the additive employed can have a dramatic impact upon the cathode kinetics. When measurements were performed on the graphite anode at 0°C, much less impact of electrolyte additive type upon the de-intercalation kinetics was observed for the graphite anodes, as illustrated in Fig. 5, being over a magnitude greater than the NCM electrodes.

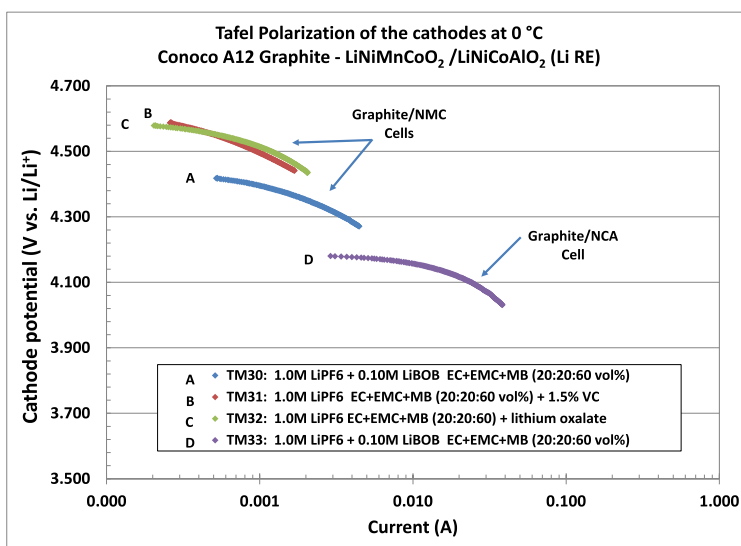


Figure 4. Tafel polarization measurements of Li_{1.2}Ni_{0.15}Co_{0.10}Mn_{0.55}O₂ (NCM) and LiNi_{0.80}Co_{0.15}Al_{0.05}O₂ (NCA) electrodes from graphite/ NCM and graphite/ NCA cells containing methyl butyrate-based electrolytes performed at 0°C.

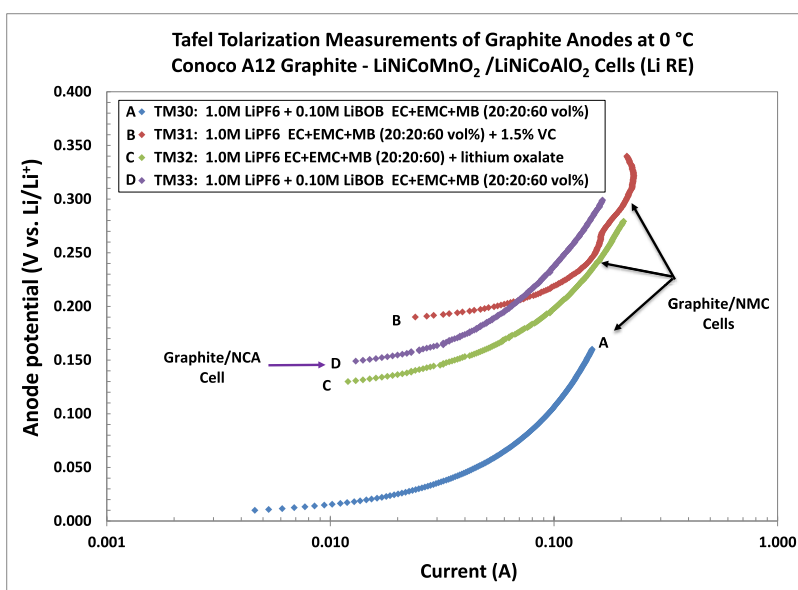


Figure 5. Tafel polarization measurements of graphite electrodes from graphite/ NCM and graphite/ NCA containing methyl butyrate-based electrolytes performed at 0°C.

EIS Measurements of Graphite/ NCM and Graphite/NCA Cells.

Electrochemical Impedance Spectroscopy (EIS) measurements were also performed on each electrode at a number of temperatures (20°, 0°, and -20°C). In general, both the NCA and NCM electrodes were observed to dominate the cell impedance. Of the different cathodes, the NCM electrodes displayed a more dramatic charge transfer resistance, which is exacerbated at lower temperatures. For example, when measurements were performed on a graphite/Li_{1.2}Ni_{0.15}Co_{0.10}Mn_{0.55}O₂ cell at 23°C containing 1.0M LiPF₆ in EC+EMC+MB (20:20:60 v/v %) + 1.5VC, as shown in Figure 6, dramatically higher charge transfer resistance is observed compared to the graphite anode (corresponding to the semi-circle arc at low frequencies). These results complement the findings of the Tafel polarization measurements well, in that the poor lithium intercalation kinetics of the NMC cathodes can be attributed to high charge transfer resistance

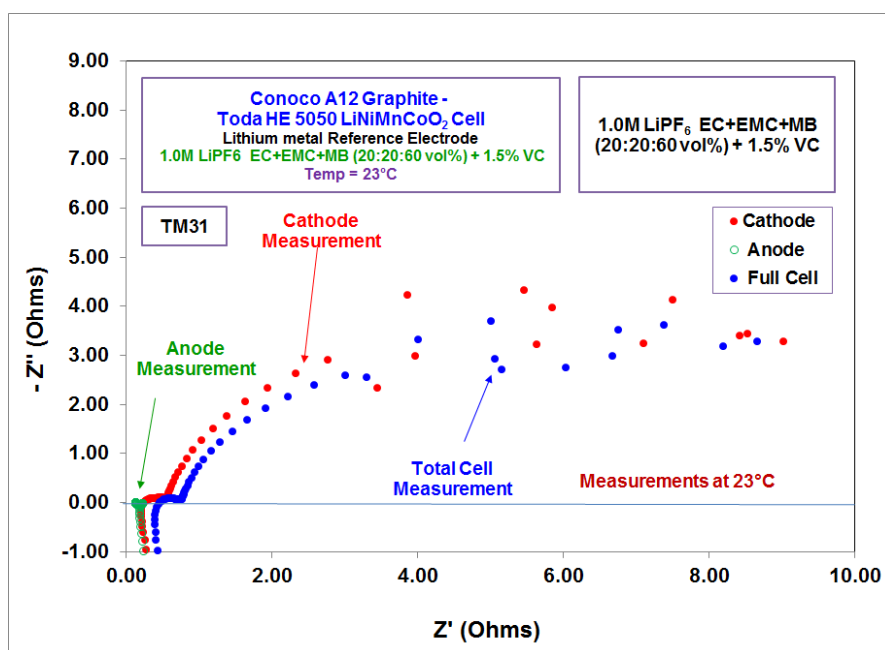


Figure 6. EIS measurements performed on a graphite/Li_{1.2}Ni_{0.15}Co_{0.10}Mn_{0.55}O₂ (NCM) cell containing 1.0M LiPF₆ in EC+EMC+MB (20:20:60 v/v %) + 1.5VC at 23°C.

Summary and Conclusions

A number of wide operating temperature range electrolyte formulations containing methyl butyrate and various additives have been investigated in Conoco Phillips A12 graphite/Toda HE5050 Li_{1.2}Ni_{0.15}Co_{0.10}Mn_{0.55}O₂ cells. When evaluated at various rates at low temperatures, the methyl butyrate-based electrolytes resulted in improved rate capability compared to a cell with an all carbonate-based formulation. Of the electrolyte investigated, the solution consisting of 1.0 M LiPF₆ + 0.10M LiBOB in EC+EMC+MB (20:20:60 v/v %) electrolyte exhibiting the best performance at low temperatures, which was attributed to a combination to good ionic conductivity and improved cathode kinetics. In general, it was determined that the cathode kinetics dominates the generally poor rate capability of this system at low temperature in contrast to traditionally used LiNi_{0.80}Co_{0.15}Al_{0.05}O₂-based systems, with

the electrolyte type having less influence. These conclusions are supported by Tafel polarization measurements, where the NCM electrodes displayed much lower lithium intercalation kinetics compared to the NCA electrodes, which is exacerbated at lower temperatures. EIS measurements further supported these findings and suggest that the charge-transfer kinetics of the cathode is particularly slow and contributes significantly to the overall cell impedance and poor rate capability. In summary, although improved low temperature performance has been demonstrated, it should be noted that the rate capability of the system (which is dominated by the slow kinetics of the NMC electrodes) is much poorer than comparable NCA-based systems, which is magnified at higher rates and lower temperatures.

Acknowledgments

The work described here was carried out at the Jet Propulsion Laboratory, California Institute of Technology, under contract with the National Aeronautics and Space Administration (NASA) and under sponsorship by the Assistant Secretary for Energy Efficiency and Renewable Energy, Office of Vehicle Technologies of the U.S. Department of Energy under Contract No. DE-AC02-05CH11231, Subcontract No 6879235 under the Batteries for Advanced Transportation Technologies (BATT) Program.

References

1. Z. Lu, D.D. MacNeil, and J. R. Dahn, *Electrochem. Solid State Lett.*, **4 (12)**, A200-A203 (2001).
2. S. -H. Kang, and K. Amine, *J. Power Sources*, **124**, 533-537 (2003).
3. S. -H. Kang, and K. Amine, *J. Power Sources*, **146**, 654-657 (2005).
4. C. S. Johnson, N. Li, J. T. Vaughey, S. A. Hackney, and M. M. Thackeray, *Electrochem. Comm.*, **7 (5)**, 528-536 (2005).
5. M. C. Smart, B. V. Ratnakumar, K. B. Chin, and L. D. Whitcanack, *J. Electrochem. Soc.*, **157 (12)**, A1361-A1374 (2010).
6. M. C. Smart, B. V. Ratnakumar, and K. Amine, 218th Meeting of the Electrochemical Society, Las Vegas, Nevada, Oct. 13, 2010.
7. M. C. Smart, B. L. Lucht, S. Dalavi, F. C. Krause, and B. V. Ratnakumar, *J. Electrochem. Soc.*, **159 (6)**, A739-A751 (2012).
8. K. A. Smith, M. C. Smart, G. K. S. Prakash, and B. V. Ratnakumar, *ECS Trans*, **16 (35)**, 33 (2009).
9. M. C. Smart, F. C. Krause, W. C. West, J. Soler, G. K. S. Prakash, B. V. Ratnakumar, *ECS Trans*, **35 (13)**, 1 (2011).
10. M. C. Smart, B. V. Ratnakumar, A. S. Gozdz, and S. Mani, *ECS Trans*, **25 (36)**, 37 (2010).
11. A. Xiao, L. Yang, and B. L. Lucht, *Electrochem. Solid State Lett.*, **10 (11)**, A241-244 (2007).
12. A. R. Armstrong, M. Holzapfel, P. Novak, C. S. Johnson, S.-H. Kang, M. M. Thackeray, P. G. Bruce, *J. Am. Chem. Soc.*, **128**, 8694 (2006).